

Production and Characterization of Ternary Heusler Shape Memory Alloy with A New Composition

O. Karaduman^a, C. Aksu Canbay^{a,*}, İ.Özkul^b, S. Aziz Baiz^a, N. Ünlü^a

^aDepartment of Physics, Faculty of Science, Firat University, Elazig 23169, TURKEY

^bMersin University, Faculty of Engineering, Department of Mechanical Engineering, Mersin/TURKEY

In this presented study, a ternary Cu-Al-Mn shape memory alloy was produced by arc melting with the new composition of Cu-23.08Al-0.5Mn (at%). The structural and thermal properties of the alloy were investigated after homogenization. The characteristic martensitic transformation temperatures of the alloy were determined by differential scanning calorimetry (DSC) measurement and the thermodynamic parameters were calculated. The differential thermal analysis (DTA) measurement was also made to see the phase transitions at high temperatures above martensitic temperature region of the alloy. Both at room temperature; the optical metallography shootings on the morphological surface of the alloy and the X-ray measurement for detecting the alloy's structural diffraction planes were made and their results showed the martensite formations of dominat M18R with very minor 2H in the alloy. All of adduced evidence manifested that this newly composed Cu-Al-Mn alloy possesses shape memory property by its martensitic phase transformation at over 100 °C, as being an HTSMA (high temperature SMA). Thereby, this new nominally composed CuAlMn alloy may be useful for the thermomechanical applications operating at this high temperature range.

Keywords: Shape memory alloy, CuAlMn, HTSMA, Martensite, Heusler alloy

Submission date: 10 March 2018

Acceptance Date: 17 April 2018

***Corresponding author:** caksu@firat.edu.tr

1. Introduction

In smart materials family, shape memory alloys (SMAs) are known as the alloys with the ability to revert back to their first preformed shape and size via a proper thermal procedure [1]. These alloys are sensitive to thermal changes or other exogenous affectional drivers like magnetic field and stress and can have two different crystal structures above and below the conversion temperatures which are the characteristic start and finish temperatures of martensite and austenite phases; M_f , M_s , A_s and A_f , from the lowest to the highest, respectively.

Among SMAs, the most commonly used SMAs are NiTi and copper (Cu) based alloys, but when compared with NiTi ones Cu-based alloys are relatively cheaper and have easier production process and some apart advantages. For example Cu-rich CuAlMn alloys, these alloys have high strength and fabulous damping capacity properties stem from their martensitic phase transformations [2, 3] and also can develop more ductility by their low degree ordered parent

$\beta 1(L2_1)$ phase due to embodying in the alloy with a low Al concentration (<18 at%) and minor amounts of Mn addition for grain refinement, phase stabilization and to decrease and surpass aluminum's brittleness effect on the matrix of Cu-rich alloy [4, 7]. Nevertheless, CuAlMn alloys have propensity for stress induced cracks due to the formation of voids during rapid cooling.

In CuAlMn SMAs, the disordered metastable β -phase becomes ordered and stable at high temperatures (after eutectoid temperature region) and these alloys show a sequence of multistep phase transitions cascading down as; disordered $\beta(A2) \rightarrow$ ordered $\beta 2(B2) \rightarrow$ eutectoid decomposition $(\alpha+\gamma 2) \rightarrow$ eutectoid recombination \rightarrow disordered $\beta 2(B2) \rightarrow$ ordered $\beta 3(L2_1)$ austenite \rightarrow monoclinic $\beta 3'$ (M18R) or $\beta 3''(\beta 3'$ plus with $\gamma 3'(2H)$) martensite during a cooling process and a shape memory effect (SME) occurs above 16 at% Al content [5-7]. Here, the $\beta 3$ of Heusler ($L2_1$) phase is a superlattice type of ordered $\beta 1(DO_3)$ superlattice phase, similarly the $\beta 3'$ and $\gamma 3'$ phases

seen in Heusler alloys are the types of $\beta 1'$ and $\gamma 1'$ martensite forms.

If aluminum content is high or electron concentration (e/a) value of the alloy becomes higher than 1.45 then the minor $\gamma 1'(\gamma 3')$ martensite forms also come explicitly into existence as interwoven with $\beta 1'(\beta 3')$ and for bigger than 1.49 then at this time the $\gamma 1'$ forms attain high dominancy over $\beta 1'$ [6, 8].

In this presented study, a ternary CuAlMn shape memory alloy with its new Cu-23.08Al-0.5Mn (at%) was produced and characterization measurements and analyses were made to obtain the thermal and structural aspects of the alloy sample to know whether it has a shape memory property whereby a martensitic transformation or not.

2. Experimental details

In order to fabricate the CuAlMn alloy according to its chemically new Cu-23.08Al-0.5Mn (at%) composition data obtained by EDX analysis, the high purity (%99.99) of Cu, Al and Mn powders were mixed in a magnetic stirrer for 3 minutes at first, then pelletized under the pressure of 1 ton and this pellet was melted under argon atmosphere by using an Edmund Buehler arc melter to obtain as cast ingot, then this ingot was cut into small pieces and heat-treated at 900 °C and immediately quenched in iced-brine water, sequentially.

To search whether the alloy possessed shape memory properties or not the differential thermal analysis (DSC and DTA) measurements were carried out to determine the characteristic martensitic transformation temperatures and kinetic parameters of the alloy by using a Shimadzu TA-60 WS. The structural XRD (by using a Rigaku RadB-DMAX II diffractometer with CuK α radiation) and optical microscopy measurements were made both at room conditions to detect the X-ray diffraction planes and morphological surface aspects of the alloy sample, respectively.

3. Results and discussion:

The curve as the result of differential scanning calorimetry (DSC) measurement performed at 15 °C/min of heating/cooling rate was given in Fig.1 and it shows the peaks of forward martensite to austenite phase (M→A) and its reverse A→M transitions of the alloy sample. On the left down heating part of this curve the downward endothermic peak at between 120-155 °C implied the forward transition from $\beta 1'$ martensite to $\beta 1(L2_1)$ austenite phase and inversely to this above there is a correspondent upward exothermic peak at between 85-130 °C indicated the reverse transition from A to M phase.

Characteristic transformation temperatures and thermodynamic parameters of the alloy were given in Table 1. The T_0 equilibrium temperature, which is at between A and M phase where their Gibbs free energies of them are equal, was calculated from the formula [9] as below;

$$T_0 = \frac{A_f + M_s}{2} \quad (1)$$

here, A_f is austenite finish and M_s is martensite start temperatures.

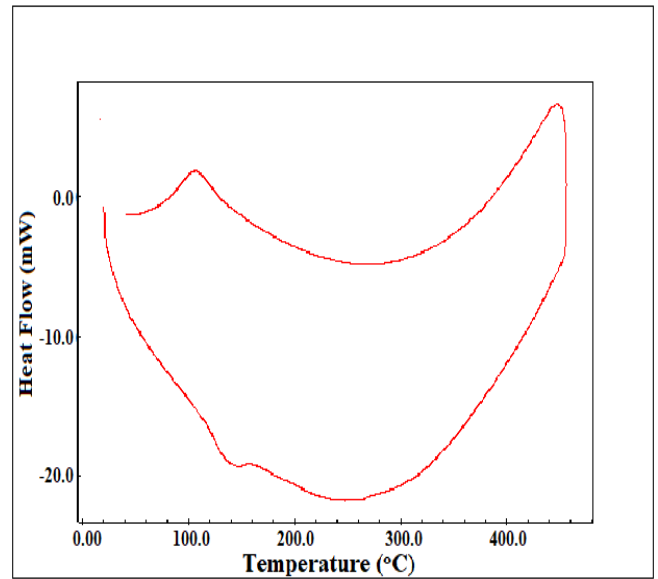


Fig.1: DSC heating/cooling cycle curve of the alloy sample.

Table 1: Values of characteristic transformation temperatures and thermodynamic parameters of the alloy.

A_s (°C)	A_f (°C)	A_{max} (°C)	M_s (°C)	M_f (°C)
120.76	155.15	146.96	130.02	85.01
T_0 (°C)	$\Delta H_{M \rightarrow A}$ (J/g)	$\Delta S_{M \rightarrow A}$ (J/g°C)	$A_s \cdot M_f$ (°C)	$A_f \cdot M_s$ (°C)
142.58	4.57	0.032	35.75	25.13

The entropy change (ΔS) during M to A transition was found from the following equation [10];

$$\Delta S_{M \rightarrow A} = \frac{\Delta H_{M \rightarrow A}}{T_0} \quad (2)$$

where ΔH is enthalpy change and its value was obtained from the DSC analysis of M to A peak. The transformation hysteresis ($A_s \cdot M_f$) value of 35.75 °C was also given in Table 1.

Furthermore, on the DTA curve as seen in Fig.2, after the first downward endothermic peak which belongs to M→A transformation, the endothermic $\beta 1 \rightarrow B2$ transition peak appears at nearly 400 °C and at the right edge of this peak the eutectoid decomposition of metastable B2 into α plus $\gamma 2$ precipitation phases and then these temporary precipitation phases dissolve by converting into a stable and B2 phase and it can be seen as the deepest endothermic peak at nearly 550 °C which is the eutectoid dissolution point of CuAlMn alloy sample and common to Cu-based SMAs.

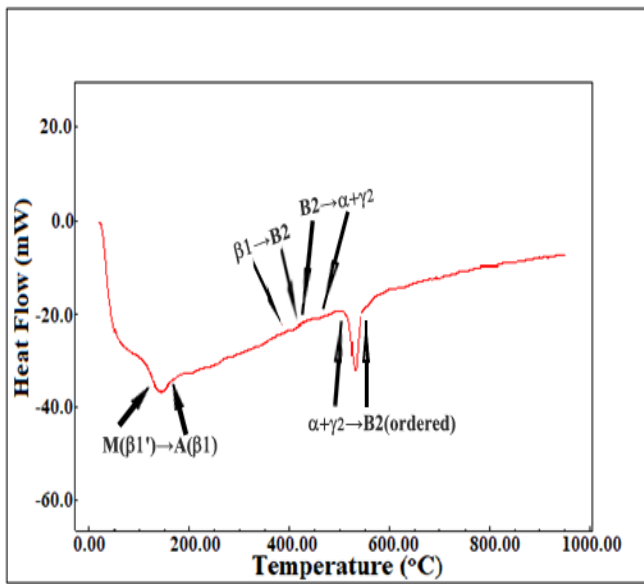


Fig.2: DTA curve of the alloy sample.

From XRD measurements at room temperature the $\beta 1'$ (M18R) martensite structures in the alloy were detected as diffracted X-ray peaks and correspondent martensite lattice planes and were displayed in Fig.3. The highest peak was observed at 46.86° which belong to (1210) plane of $\beta 1'$ martensite and the other appeared planes of $\beta 1'$ peaks are (122), (0022), (128), (222), (042) and (211) planes [11-13].

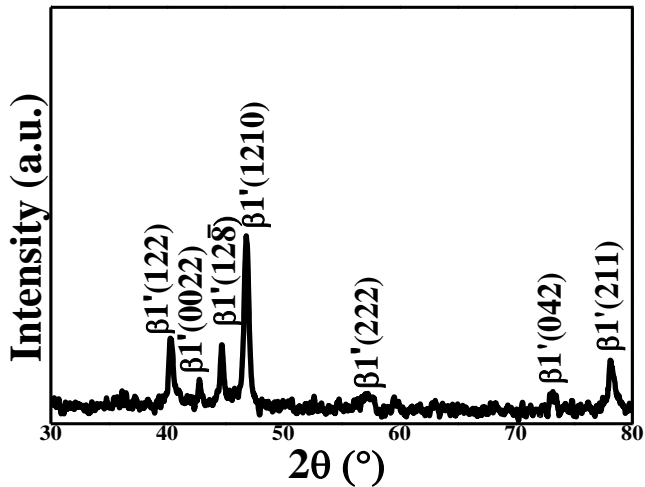


Fig.3: X-Ray diffraction peaks and correspondent martensite planes of the CuAlMn alloy.

The average crystallite size (D) of the alloy was calculated by using Debye-Scherrer [14, 15] formula;

$$D = \frac{0.9\lambda}{B_{1/2} \cos \theta} \quad (3)$$

here, λ is CuK α -X-ray wavelength ($\lambda=0.15406$ nm), B is FWHM (full width at half maximum) of the highest peak and θ is Bragg angle. Thus D was found as 21.12nm and thinking

this small size as one dimensional line it may contain a chain of nearly 50 copper atoms. As seen in Eq.3, if the B width of the highest peak becomes broader then the D crystallite size of the alloy decreases and this means that the surface areas so the numbers of linear defects (dislocations) in the polycrystalline alloy increase and these increments generally improve the shape memory and ductility properties of the alloy.

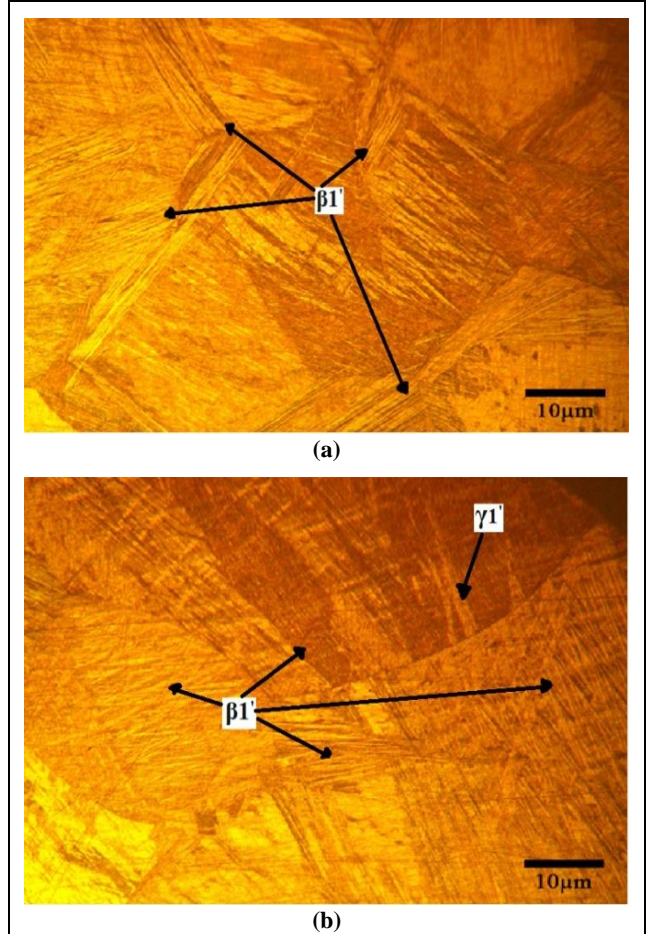


Fig.4: The optical micrographs of the CuAlMn alloy: a) one shot and b) another shot.

In SMAs, the martensitic transformations caused by heating/cooling processes (in which the vibrational entropy is changed) are first order, and diffusionless. The vibrational entropy change (ΔS) of average periodic lattice formation is a function that is too closely depended on valence electron concentration (e/a). The valence electron/atom concentration of an alloy system is very important to have shape memory property. The valence electron concentration per atom in the alloy, i.e. the e/a rate was found by the formula [16] as below;

$$\frac{e}{a} = \sum f_i v_i \quad (4)$$

where f_i represents the atomic fractions of each element of the alloy and v_i is correspondent numbers of valence electrons. In this work, the e/a ratio of CuAlMn sample was found as 1.46 and this value implies that the dominant phase

should be the forms of $\beta 1'$ martensite phase. The proofs supporting to this hypothesis can be seen in Fig.4-a and b as optical micrography images displaying the martensite forms existed on the surface morphology of CuAlMn sample. In Fig.4-b the minor $\gamma 1'(2H)$ martensite which is caused from high amount of Al content was also observed [17].

Conclusions

The thermal and structural measurements of newly composed CuAlMn shape memory alloy with high amount of Al and minor Mn were made after its production via arc melting. By the DSC analysis of the alloy, the characteristic martensite start (130°C) and austenite start (120°C) temperatures were determined as entwined together and the kinetic parameters were also calculated, the transformation hysteresis was found as $\sim 35^{\circ}\text{C}$. The DTA curve depicted that the alloy had a multi-stage phase transitions of $\beta 1'(18R)$ martensite $\rightarrow \beta 1(L2_1$ -Heusler) austenite $\rightarrow \beta 2(B2)$ under heating way, as this process is common to CuAlMn alloys. At room conditions, XRD results revealed the $\beta 1'(M18R)$ martensite plane peaks and the formations of this martensite phase with minor $\gamma 1'(2H)$ were also able to be seen by naked eye on the optical micrographs of the alloy as real morphological semblances. In conclusion, this new CuAlMn shape memory alloy may be useful in various thermomechanical applications in compliance with its physical SMA properties.

Acknowledgements

This study was financially supported by the Research Fund of Mersin University in Turkey with the project number 2018-1-AP1-2839.

References:

- [1] K. Otsuka and C. Wayman, Shape memory materials (Cambridge University Press, 1998): pp.xiii-5.
- [2] Arlic et al. Impact of Alloy Composition and Thermal Stabilization on Martensitic Phase Transformation Structures in CuAlMn Shape Memory Alloys. Materials Research, (2018); 21(suppl. 2): e20170897. <http://dx.doi.org/10.1590/1980-5373-mr-2017-0897>
- [3] C.A. Canbay. Int J Thermophys (2015) 36:783–794. <https://doi.org/10.1007/s10765-015-1842-2>
- [4] Y. Sutou, R. Kainuma, K. Ishida, Mater. Sci. Eng. A 273–275, (1999), 375–37. [https://doi.org/10.1016/S0921-5093\(99\)00292-0](https://doi.org/10.1016/S0921-5093(99)00292-0)
- [5] R. Kainuma, N. Satoh, X.J. Liu, I. Ohnuma, K. Ishida, J. Alloys Comp. 266, 191 (1998). [https://doi.org/10.1016/S0925-8388\(97\)00425-8](https://doi.org/10.1016/S0925-8388(97)00425-8)
- [6] M.O. Prado, et al., Martensitic Transformation In Cu-Mn-Al Alloys. Scripta Metallurgica et Materialia, Vol. 33, No. 6: pp.877-883, (1995). DOI: [10.1016/0956-716X\(95\)00292-4](10.1016/0956-716X(95)00292-4)
- [7] U.S. Mallik, V. Sampath, J. Alloys Compd. 459: 142-147(2008). <https://doi.org/10.1016/j.jallcom.2007.04.254>
- [8] J. Pelegrina, M. Ahlers, The martensitic phases and their stability in Cu-Zn and Cu- Zn- Al alloys-I. The transformation between the high temperature β phase and the 18R martensite. Acta Metall. Mater. 40: 3205–3211, (1992). [https://doi.org/10.1016/0956-7151\(92\)90033-B](https://doi.org/10.1016/0956-7151(92)90033-B)
- [9] R.J. Salzbrenner, M. Cohen, On the thermodynamics of thermoelastic martensitic transformation. Acta Metall., 27: 739-748, (1979). [https://doi.org/10.1016/0001-6160\(79\)90107-X](https://doi.org/10.1016/0001-6160(79)90107-X)
- [10] C.A. Canbay, Effects of Annealing Temperature on Thermomechanical Properties of Cu-Al Ni Shape Memory Alloys Int. J. Thermophys., 34(7): 1325-1335, (2013). <https://doi.org/10.1007/s10765-013-1486-z>
- [11] C. Aksu Canbay, Z. Karagoz, F. Yakuphanoglu. Acta Physica Polonica A, Vol. 125: pp.1163-1166 (2014). DOI: <10.12693/APhysPolA.125.1163>
- [12] U.S.Mallik, V. Sampath. Materials Science and Engineering A 478: 48–55, (2008). <https://doi.org/10.1016/j.msea.2007.05.073>
- [13] R. Kainuma et al. Journal of Alloys and Compounds, 266: 191–200, (1998). [https://doi.org/10.1016/S0925-8388\(97\)00425-8](https://doi.org/10.1016/S0925-8388(97)00425-8)
- [14] A. Patterson, "The Scherrer Formula for X-Ray Particle Size Determination". Phys. Rev. 56 (10): 978–982, (1939). DOI:<https://doi.org/10.1103/PhysRev.56.978>
- [15] E.Obrado, et al. Physical Review B, Vol.56(1): pp.20-23, (1997). <https://doi.org/10.1103/PhysRevB.56.20>
- [16] K. Otsuka and C. M. Wayman, Shape Memory Materials. Cambridge University Press, Cambridge, UK,(1998).
- [17] U.S. Mallik, V. Sampath. Journal of Alloys and Compounds, vol.469: pp.156–163, (2009). <https://doi.org/10.1016/j.jallcom.2008.01.128>